

Shell Models on Recurrent Sequences: Fibonacci, Padovan and Other Series

L. Manfredini, Ö. D. Gürçan

*Laboratoire de Physique des Plasmas, CNRS, Ecole Polytechnique, Sorbonne Université,
Université Paris-Saclay, Observatoire de Paris, F-91120 Palaiseau, France*

A new class of shell models is proposed, where the shell variables are defined on a recurrent sequence of integer wave-numbers such as the Fibonacci or the Padovan series, or their variations including a sequence made of square roots of Fibonacci numbers rounded to the nearest integer. Considering the simplest model, which involves only local interactions, the interaction coefficients can be generalized in such a way that the inviscid invariants, such as energy and helicity, can be conserved even though there is no exact self-similarity. It is shown that these models basically have identical features with standard shell models, and produce the same power law spectra, similar spectral fluxes and analogous deviation from self-similar scaling of the structure functions implying comparable levels of turbulent intermittency. Such a formulation potentially opens up the possibility of using shell models, or their generalizations along with discretized regular grids, such as those found in direct numerical simulations, either as diagnostic tools, or subgrid models. It also allows to develop models where the wave-number shells can be interpreted as sparsely decimated sets of wave-numbers over an initially regular grid. In addition to conventional shell models with local interactions that result in forward cascade, a particular helical shell model with long range interactions is considered on a similarly recurrent sequence of wave numbers, corresponding to the Fibonacci series, and found to result in the usual inverse cascade.

I. INTRODUCTION

Turbulence represents one of the most challenging problems in nonlinear physics, with applications ranging from fluid dynamics and plasma physics to ocean currents and atmospheric dynamics. One of its key intrigues is that despite the presence of spatio-temporal chaos across a wide range of scales it nonetheless exhibits order, specifically in the form of self-similarity of its hierarchy of spatial structures, encapsulating the concept of restored statistical symmetry [1, 2]. Consequently, one of the main lines of inquiry in turbulence research, is that of the study of the turbulent fluid as a non-equilibrium steady state with energy injection and dissipation at well separated scales and a nonlinear transfer in between those, in a so-called inertial range, resulting in power law solutions for the turbulent spectra and intermittency of the statistics of its fluctuations [1, 3].

One of the main branches of academic research on turbulence is dedicated to development of reduced models [4], focused on various reduction strategies hoping to find one that reduces the system to a tractable problem without losing any essential features. In this context, shell models [5–9] appear as one of the simplest yet most prominent examples of such models. Notably, shell models have been used for understanding certain complex aspects of turbulence, such as multifractality [10–13], which are too difficult to tackle using the full Navier-Stokes equations. Additionally, these low-dimensional dynamical systems have shown their versatility in modeling other systems like rotating turbulence [14], passive scalar advection [15] and convection [16]. Beyond fluid turbulence, shell models have been used to study the nature of cascades in magnetohydrodynamic (MHD) turbulence [17, 18], including the transition from weak to strong cascade in reduced MHD [19]. In the context of

fusion plasma, they have also been applied to study the L-H transition using multi-shell models [20].

In their general form, shell models consist of a set of ordinary differential equations for a set of variables corresponding to a group of wave-numbers that retain only the essential characteristics of the original equations—namely, the quadratic nonlinearity, the scale invariance, and a resulting set of quadratic conserved quantities. These models can reproduce some of the key features of fully developed 3D turbulence, such as the power law exponents of the turbulent cascades and the intermittency of their fluctuations [21, 22]. They are usually written in a desired form where the coefficients are computed using the constraints imposed by the conservation laws instead of being derived from the original system of equations.

Alternatively, shell models can be seen as a simultaneous reduction of the wave-number domain using a set of logarithmically spaced wave-numbers $k_n \sim k_0 g^n$, and the nonlinear interaction operator by reducing the number of possible interactions in the convolution integral to a finite set of -usually local- interactions. Historically, a complex variable u_n is used to represent the Fourier modes in the shell n which contains the wave-numbers between k_n and k_{n+1} with a constant inter-shell ratio g , -usually chosen to be equal to 2, which would interact nonlinearly with the two neighboring shells on both sides. However choosing $g = 2$ is somewhat problematic, because since it is impossible to have $\mathbf{k}_n + \mathbf{k}_{n+1} + \mathbf{k}_{n+2} = 0$ with $g = 2$, which means that the cell centers do not interact, and the interactions that are described in such a shell model come only from the parts of the shells that are close to the boundaries between the consecutive shells. In other words $g = 2$ produces shells that are in fact too large to keep track of where the energy actually goes.

This is also not ideal for establishing the connection between the shell model and Fourier space decimation

as in the case of spiral chain models for example [23], which incidentally gives exactly the same equations as shell models, but only with g values that permit triadic interactions, such as $g = \sqrt{\varphi}$ where φ is the golden ratio. Note that $g=\varphi$ is the largest possible value for shell spacing if one wants to use Fourier space decimation with actual triadic interaction between cell elements.

More generally, the use of logarithmic discretization, used in shell models, but also in other reduced descriptions such as logarithmically discretized models [24], log-lattice models [25–27] or spiral chains [23], allows covering a large range of scales using a small number of degrees of freedom, providing an important advantage over direct numerical simulations on regular Fourier space grids, such as those in pseudo-spectral codes. However apart from $g = 2$, which we argue to be dubious, the discretized wave-numbers k_n , do not fall on regular grid elements. This means that if we start from a regular Fourier space grid, and construct a reduced model of this type, which has the mathematical form of a shell model (including log-lattice models), the shell elements which would have $k_i = \{1, \varphi, \varphi^2, \varphi^3, \dots\}$ etc. do not fall on regular grid points. In order to remedy this, here we propose a shell model like discretization, but on a set of wave-numbers that follow a recurrent sequence such as the Fibonacci series (skipping the first two elements in order to have the same structure as a shell model): $k = \{1, 2, 3, 5, \dots\}$. Note that eventually the Fibonacci sequence converges to the above geometric sequence, and we get the usual progression with spacing approximately equal to the golden ratio $g \approx \varphi$ for large values of n .

Even though the Fibonacci series allows each wave-vector in a sequence to be the sum of the two precedent wave-vectors, and as such it allows each shell to interact with every part of the two consecutive shells as opposed to the $g = 2$ case, it does not *really* allow triadic interactions between cell centers since the area of such a triad and thus its interaction coefficient vanishes. In order to remedy this, we have also considered the Padovan sequence. Three consecutive wave-numbers that follow a Padovan sequence can actually form triads, (asymptotically with the angles, $\theta_{kp} \approx 97.04^\circ$, $\theta_{kq} \approx 34.44^\circ$ and $\theta_{pq} \approx 48.52^\circ$), even though a chain of such triads does not *a priori* fall on regular grid points, since it is the absolute values of the wave-numbers that are integers. Note that if one generalizes this idea to two or three dimensions for example using log-lattice models or spiral chains, the wave-number sequences would represent separate components $k_n^{(x,y,z)}$ (or $k_n^{(r,\theta)}$ etc.). For example, in the case of log-lattices, such wave-number sequences would naturally form triads since it is the components that satisfy the recurrence relations. In this sense, even though we focus on shell models here, the idea of using recurrent sequences to replace logarithmic scaling is very general and applicable to all kinds of models and systems, including log-lattices [26] where the components can be written as g^n where g is a special ratio such as the golden ratio, or the plastic ratio (by the way, one

can add the supergolden ratio to that list) or the nested polyhedra models [28, 29] where the x, y, z components of the vertex positions of the initial regular polyhedra can be rearranged to be written in terms of various combinations of $0, 1, \pm\varphi, \pm\varphi^2$ so that exact triadic interactions are possible. In all these cases, considering a recurrent sequence will transform the logarithmic scaling to the corresponding recurrent series, while keeping the triadic interactions intact.

We observe that a scaling of $g = \sqrt{\varphi}$ also allows to form actual triangles, with a non-zero area, leading us to also consider the sequence of numbers that consist of the square roots of the Fibonacci numbers rounded to the nearest integer as an alternative sequence. In contrast to those series that satisfy additive recurrence relations, this series satisfy a recurrence relation for the squares of the wave-number magnitudes. As such this series would be more suitable for a logarithmically discretized model (where the discretization is logarithmic in k and linear in θ in polar coordinates) as opposed to a log-lattice where the discretization is logarithmic in Cartesian coordinates.

We further considered variations and combinations of these sequences, and generally observed that shell models on recurrent integer sequences behave virtually identically to conventional shell models. Some of the proposed sequences may be linked to particular elements of a regular grid based on different geometric constructions. For example, the Fibonacci spiral can be used to span a 2D Fourier space in a particular way, by sequentially adding squares whose sides are represented by Fibonacci numbers. Likewise, we can construct a similar spiral in 3D Fourier space, the Padovan cuboid spiral, based on a sequence of cuboids, with integer dimensions. Thus, it is possible to establish different connections between a shell model, defined by such a recurrent sequence of vectors k_n and a regular Cartesian grid.

The rest of the paper is organized as follows: In Sec. II, we present the GOY model revisited in order to conserve the inviscid invariants on an arbitrary wave-number sequence. In Sec. IIA, we introduce various asymptotically self-similar sequences and discuss their corresponding geometric properties. Sec. IIB compares the results between asymptotically self-similar sequences and respective self-similar ones. An intermittency analysis is conducted in Sec. IIC demonstrating its dependence on inter-shell spacing. Additionally, Sec. IID presents a further test of the model implemented on a wave-number sequence that is not asymptotically self-similar, i.e. a sequence compound in which the ratio between two consecutive term alternates. In Sec. III, we introduce the helically decomposed shell model, implemented on a generic wave-number sequence. Finally, conclusions are presented in Sec. IV.

II. GOY MODEL ON A RECURRENT SEQUENCE

Let us consider a generic, shell model:

$$\frac{du_n}{dt} = i \sum_{\Delta} \Lambda_{nm\ell} u_m^* u_\ell^* - d_n u_n + f_n, \quad (1)$$

where u_n is a complex variable representing the dynamics of the velocity field at a given wavelength k_n , f_n represents external forcing and $d_n = \nu k_n^{2p} + \mu k_n^{-2q}$ is the general form of (hyper/hypo)-viscosity. The forcing is usually taken to be localized to a given shell $n = n_f$ or a few shells around it, whereas the nonlinear term $\sum_{\Delta} \Lambda_{nm\ell} u_m^* u_\ell^*$ models the nonlinear interactions between shell variables, representing a reduced subset of all the triadic interactions in Fourier space. As a particular example that retains only local interactions the GOY model [30] can be written as:

$$\begin{aligned} \sum_{\Delta} \Lambda_{nm\ell} u_m^* u_\ell^* = & \left[(k_{n+2} + k_{n+1}) u_{n+2}^* u_{n+1}^* + \right. \\ & \left. + (k_{n-1} - k_{n+1}) u_{n-1}^* u_{n+1}^* - (k_{n-1} + k_{n-2}) u_{n-1}^* u_{n-2}^* \right], \end{aligned} \quad (2)$$

where the coefficients are chosen such that the nonlinear term conserves the usual quadratic quantities without any assumptions regarding the self-similar nature of the shell variables. The conserved quantities in question, are the two inviscid invariants that characterize 3D Navier-Stokes turbulence, namely energy and helicity, defined as follows:

$$E = \sum_n |u_n|^2, \quad H = \sum_n (-1)^n k_n |u_n|^2. \quad (3)$$

In this formulation, similar to the original GOY model, the shell variables, carry either positive or negative helicity, depending on whether n is even or odd. It can be shown that in the limit of constant shell spacing $k_n = k_0 g^n$, the present model reduces to the usual form of the GOY model [30] of 3D turbulence. Choosing the phase relation typical of the Sabra model, we can also obtain the Sabra [7] version of this model. The premise of this paper is that, since Eqs. (1) and (2) work on any sequence of wave-numbers, we can use them on a series of wave-numbers that are on an arbitrary sequence of integers, focusing in particular on recurrent sequences (i.e. the sequences that we can obtain from a recurrence relation). We can then study the spectra obtained from shell models on these recurrent sequences in order to characterize the effects of non-exact self-similarity on the resulting wave-number spectra, spectral fluxes and intermittency. One can imagine a scenario, for example, where the breaking of the exact self-similarity symmetry of the

system would result in a different kind of multifractality. In the article ‘‘Shell Model Intermittency as Hidden Self-Similarity’’ [31], Mailybaev asserts that intermittency is related to hidden self-similarity, while Aumaître et al. [32] present intermittency as a consequence of a stationarity constraint on energy flux, demonstrating that under this assumption, the fluctuations of the energy flux are characterized by scaling exponents consistent with the She-Leveque formula [33]. The shell model presented in this article can be implemented on a self-similar grid, an asymptotically self-similar grid, or a non-self-similar sequence of wave numbers, providing a potential framework to test these ideas by relaxing explicit, built-in self-similarity of the conventional shell models.

A. Recurrent Sequences

Since the primary goal of this paper is to demonstrate how the proposed model can reproduce standard shell model features without strict self-similarity, we follow the approach of selecting different integer sequences, representing shell elements that lie on a regular grid and approach a constant inter-shell spacing. In order to achieve an asymptotic ratio between consecutive terms, we choose sequences defined through recurrence relations. Note that the asymptotic ratio is entirely determined by the solution of the characteristic equation derived from the recurrence relation (e.g., $x^2 = x + 1$ for the Fibonacci sequence), rather than by the initial terms. This approach provides us with a variety of sequences on which the model can be implemented and compared with their corresponding self-similar counterparts. Below, we list the various asymptotically self-similar sequences that we have used.

Note also that, using recurrent sequences also have applications in the context of anisotropic shell models, including multi-branch shell models [23], and in the recent work of Ref. [34] that introduce a shell model for resonant wave interactions where the frequencies follow the Fibonacci sequence: the resonant manifold condition is ensured by the recurrence relation, i.e. involving resonances between three consecutive modes. In addition to all the specific choices presented below, which we will investigate numerically, it is worth mentioning that given any desired inter-shell spacing g , it is also always possible to construct an asymptotically self-similar sequence of integers defined by $k_n = \lfloor k_0 g^n \rfloor$, which rapidly converges to constant inter-shell spacing.

Another point is that the conventional GOY model with $g = 2$, also happens to be an integer sequence that one can call the ‘‘powers of two’’ sequence. It is immediately self-similar and can be viewed as a recurrent series with the recurrence $k_n = 2k_{n-1}$. In this sense, one may argue that the natural generalization of the GOY model with $g = 2$, is to recurrent series instead of non-integer g values.

1. Fibonacci and Lucas sequences

Starting with $k_0 = 0$ and $k_1 = 1$, and constructing the rest of the sequence using the Fibonacci recurrence relation $k_n = k_{n-1} + k_{n-2}$, we obtain the Fibonacci numbers. Alternatively, starting with $k_0 = 2$ and $k_1 = 1$, with the same recurrence relation, we get the Lucas numbers. The asymptotic inter-shell spacing of both sequences is determined by the characteristic polynomial, whose solution gives us the asymptotic inter-shell ratio as the golden ratio φ .

Since φ is the maximum possible value for k_n that forms a triangle with k_{n-1} and k_{n-2} , (albeit a flat one), it can be used as a natural boundary for the shells, where the shell centers barely interact. It also works nicely for components of a log-lattice, which can be seen as a multi-dimensional generalizations of shell models. Given this recurrence relation, it is also possible to assign a geometric significance to the sequence. For instance, the Fibonacci and Lucas spirals can be constructed simply by adding a series of squares recursively, representing a specific partition of the 2D Fourier space on a regular grid. More generally, using an integer sequence guarantees that the shell boundaries, or centers as one may choose coincide with grid points on each of the axes.

2. Narayana sequence

The Narayana sequence is defined by the third-order recurrence relation, $k_n = k_{n-1} + k_{n-3}$. The first few terms are $k_0 = k_1 = k_2 = 1$. thereby the asymptotic inter-shell spacing is represented by the real root of the equation $x^3 = x^2 + 1$, yields the supergolden ratio $\psi \simeq 1.46557\dots$. From a geometric perspective, unlike the Fibonacci series, this sequence allows the existence of genuine triads between shell centers. Specifically, the sides of the triangle formed by these centers have lengths 1, $1/\psi$, and ψ , representing a triangle with an obtuse angle θ_{kp} of 120 degrees (with $\theta_{kq} = 23.78^\circ$ and $\theta_{pq} = 36.22^\circ$ using the convention $p < k < q$). The shell model implemented on this sequence can also be interpreted as a chain of interacting modes, connected by triads that follow this shape. Even though here we propose a local shell model for this sequence, the generalization to log-lattices would involve non-local interactions between the wave-numbers that satisfy the recurrence relations.

3. Padovan and Perrin sequences

Considering the recurrence relation $k_n = k_{n-2} + k_{n-3}$, which corresponds to the characteristic equation $x^3 = x + 1$, we obtain sequences that asymptotically approach a spacing with the plastic ratio $\rho \approx 1.324718$, which is the real root of the characteristic equation. Starting with $k_0 = k_1 = k_2 = 1$ we obtain the so-called Padovan

sequence. Alternatively starting with $k_0 = 3$, $k_1 = 0$, $k_2 = 2$, one obtains the Perrin sequence. As in the case of Narayana sequence, the log-lattice generalization would involve using the recurrence relation at each direction, where the triadic interactions would be between those wave-numbers that satisfy the recurrence relation for their components.

Similar to the Fibonacci spiral, there exists a spiral construction for the Padovan numbers, which consists of equilateral triangles whose side lengths follow the Padovan sequence. Alternatively, in 3D Fourier space, a spiral structure can be constructed by joining the diagonals of the faces of successive cuboids added to an initial unit cuboid, which is called the Padovan cuboid spiral. In this, the third dimension of each cuboid corresponds to a successive term in the Padovan sequence, while the other two dimensions match the length and width of the face being extended. The sequence starts with a $1 \times 1 \times 1$ cuboid, followed by another $1 \times 1 \times 1$ cuboid, then a $1 \times 1 \times 2$, and next a $2 \times 2 \times 3$ cuboid. Similar to the Fibonacci spiral for the 2D grid, the Padovan cuboid spiral can be considered as a specific partition of the 3D Fourier space, whose the elements lie on a regular grid, forming a chain of interacting nodes. This construction also results in a series of triangles, each defined by two sides of successive Padovan numbers with the angles $\theta_{kp} \approx 97.04^\circ$, $\theta_{kq} \approx 34.44^\circ$ and $\theta_{pq} \approx 48.52^\circ$ between these sides (with the convention that $p < k < q$).

4. Square root of the Fibonacci sequence

As we have noted, the Fibonacci series can be used as shells in k -space, but if one wants to consider them as Fourier space decimations with k_n representing magnitudes, they basically form only flat triangles. In order to generate self-similar spiral-like structures, one can instead consider a right angled triangle with two legs of length 1 and $\sqrt{\varphi}$, so that the hypotenuse would be φ . Repeating this procedure, we can obtain a model where the shell spacing is the square root of the golden ratio.

In order to force such a construction on an integer sequence, we consider the square roots of Fibonacci numbers, where a recurrence relation can be defined as $k_n = \lfloor \sqrt{k_{n-1}^2 + k_{n-2}^2} \rfloor$, starting with $k_0 = 1$, and $k_1 = 2$. Since the recurrence relation involves rounding, this is more like a numerical integer sequence. Nonetheless it is fundamentally different from simply $k_n = \lfloor k_0 g^n \rfloor$ with $g = \sqrt{\varphi}$, even though both converge to the same asymptotic ratio.

B. Self-similar vs. Recurrent Sequences

The model presented above, given N shells corresponding to a sequence of wave-numbers k_n , represents a system of N coupled ordinary differential equations (ODEs).

	k_n	N	
F_n	$k_n = k_{n-1} + k_{n-2}$	$\{0, 1, \dots\}$	36
L_n	$k_n = k_{n-1} + k_{n-2}$	$\{2, 1, \dots\}$	36
$g = \varphi$	$k_n = \varphi^n$		36
N_n	$k_n = k_{n-1} + k_{n-3}$	$\{1, 1, 1, \dots\}$	46
$g = \psi$	$k_n = \psi^n$		46
P_n^a	$k_n = k_{n-2} + k_{n-3}$	$\{1, 1, 1, \dots\}$	59
P_n^e	$k_n = k_{n-2} + k_{n-3}$	$\{2, 0, 1, \dots\}$	59
$g = \rho$	$k_n = \rho^n$		60
F_n^s	$k_n = \lfloor \sqrt{k_{n-1}^2 + k_{n-2}^2} \rfloor$	$\{1, 2, \dots\}$	67
$g = \sqrt{\varphi}$	$k_n = \sqrt{\varphi^n}$		67
C_n	$F_n \cup L_n$		68

Table I. The table sums up various integer wave-number sequences used in the numerical integrations, where the recurrence relation and the initial values are shown, as well as the scaling factors for their self-similar counterparts. In practice, the first elements of the series are regularized, meaning zeros are skipped and repetitions are avoided. The number of shells reported in the last column are chosen in order to have roughly the same range of wave-numbers with a constant value of $\nu = 5 \cdot 10^{-10}$ across all the models.

In accordance with the literature on the standard GOY model and the goal of estimating the intermittency corrections, we drive the system with a constant large-scale forcing $f_n = (1 + i\sqrt{5}) \cdot 10^{-1}$ acting on the fourth shell (i.e. $n_f = 4$), and a small scale dissipation of the form $d_n = \nu k_n^2$, with a small enough viscosity to dissipate energy only in the last few shells. Although not explicitly discussed in this section, the implementation of a forcing that is delta-correlated in time is straightforward, and does not alter the results presented here qualitatively. In order to integrate the system numerically we used a 4th order Implicit-Explicit (IMEX) solver [35, 36] in Julia [37], which allows for efficient separation of the stiff and non-stiff components of the equations.

We choose our sequences of wave-numbers so that they span seven decades in k . This allows for sufficient extension of the inertial range and is consistent with previous studies [7, 21, 22]. This corresponds to $N = 36$ shells for the Fibonacci sequence, while for the Padovan and the square root of Fibonacci numbers sequences, this corresponds to $N = 60$ and $N = 67$ shells respectively. In contrast, the conventional inter-shell ratio $g = 2$, covers seven decades with $N = 25$ shells. The parameters for all other sequences considered are summarized in the table I. We also chose to fix the dissipation at $\nu = 5 \cdot 10^{-10}$.

The system was integrated until its total energy reached a steady state, from an initial condition of small amplitude (10^{-8}) white noise, and then continued over approximately 2,000 eddy turnover times ($\tau_E^{-1} \sim k_n u_n$) of the largest scale after reaching steady state. The sampling time is set to $\delta t = 10^{-4}$, ensuring a sufficiently high

sampling rate to resolve the temporal dynamics within the inertial range. All spectral quantities are averaged over this steady state time window, as represented by $\langle \cdot \rangle$. Recall that, since the spectral energy is defined as $E(k_n) = k_n^{-1} |u_n|^2$ for shell models, a scaling of the form $|u_n|^2 \sim k^{-2/3}$ is consistent with the Kolmogorov spectrum for the forward energy cascade.

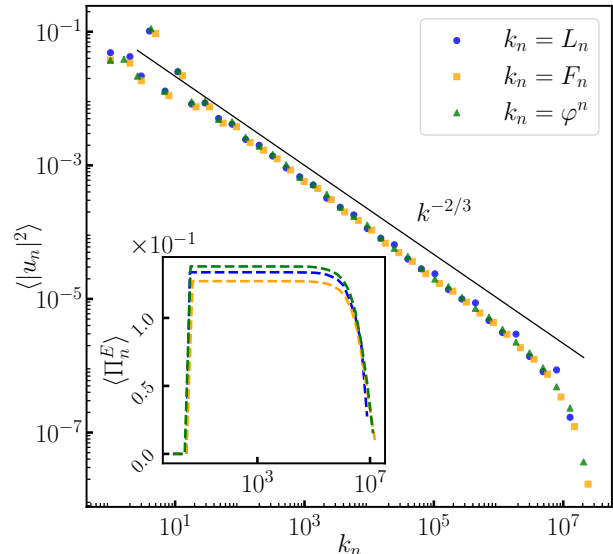


Figure 1. Log-log plot of the spectral energy for each shell $\langle |u_n|^2 \rangle$ as a function of the wave-number k_n , with the wave-numbers corresponding to the Fibonacci numbers, Lucas numbers and the respective self-similar spacing $k_n \propto \varphi^n$. In the inset, a semi-log plot shows the spectral energy flux $\langle \Pi_n^E \rangle$, defined in Eq. (4), as a function of the wavenumber k_n (log scale).

In Figure 1, the shell energy $|u_n|^2$ for the shell model implemented on the Fibonacci and Lucas sequence is compared to the respective self-similar model (i.e. with $k_n = \varphi^n$). We note that the spectrum exhibited by the two asymptotically self-similar sequences is in very good agreement with the Kolmogorov scaling and that of a GOY model with $g = \varphi$.

Following the standard GOY model definition, the spectral energy flux at a given shell k_n can be written as:

$$\Pi_n^E = 2Im((k_{n+2} + k_{n+1}) u_n^* u_{n+1}^* u_{n+2}^* + (k_n + k_{n-1}) u_{n-1}^* u_n^* u_{n+1}^*) \quad (4)$$

Note that the spectral energy flux, shown in the inset plot of Figure 1, remains perfectly constant in the inertial range both for the GOY model with $g = \varphi$ and the shell model on the Fibonacci and Lucas sequences. We observe that the level or energy flux is slightly different between the three sequences. This is because of the fact that since we force the 4-th shell in each case, which corresponds to a different wave-number in each sequence, which results in different levels of energy injection.

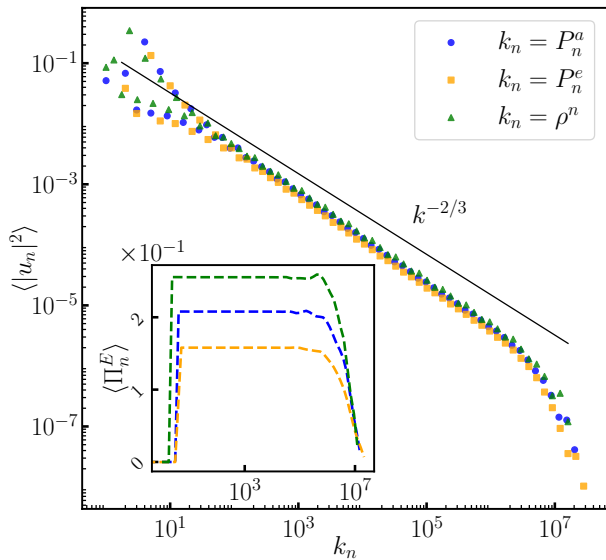


Figure 2. Log-log plot of the spectral energy for each shell $\langle |u_n|^2 \rangle$ as a function of the wave-number k_n , for a wave-number sequences corresponding to the Padovan numbers, Perrin numbers and the respective self-similar spacing $k_n \propto \rho^n$. The inset semi-log plot displays the spectral energy flux as a function of the wave-number k_n (log. scale).

As we can see in Fig. 2, the same is true also for the shell models with $g = \rho$ (i.e. the plastic ratio) and the corresponding integer sequences that approach this scaling. For the sake of brevity, we do not present the comparison between the self-similar sequence corresponding to $g = \psi$ (i.e. the supergolden ratio) and the Narayana sequence, which exhibit behavior similar to the other cases presented.

The same comparison can be repeated between the GOY model with $g = \sqrt{\varphi}$, and the associated sequence made of square roots of Fibonacci numbers rounded to the nearest integers. Again, the conclusion is that the two models behave very similar to one another, as can be seen from the plot of the spectral energy (Fig. 3). One notable observation is that the amplitude of the oscillations at the forcing scale seems to be larger, for smaller spacing, i.e. Plastic ratio and square root of golden ratio, compared to the Fibonacci case, before eventually reaching a specific scaling corresponding to a constant flux in the inertial range, as illustrated in the Figure 3. At the Kolmogorov scale, for smaller spacing, the flux presents some oscillations compared to the Fibonacci case. We also observe that the energy spectrum starts to shows slight deviations from the Kolmogorov scaling, suggesting the presence of higher-order corrections.

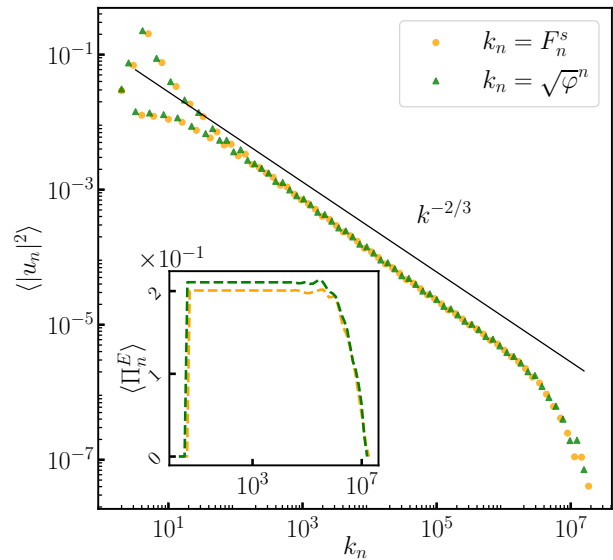


Figure 3. Log-log plot of the energy spectra for the square root of the Fibonacci sequence and the corresponding self-similar sequence. The inset semi-log plot displays the spectral energy flux as a function of the wave-number k_n (log. scale).

C. Intermittency analysis

It is well-known that the higher order structure functions computed from shell models (i.e. $S_p \equiv \langle |u_n|^p \rangle$), with the usual value of $g = 2$, exhibit deviations from the Kolmogorov scaling of $S_p \propto k_n^{-p/3}$, demonstrating intermittency [21, 22, 38, 39], somehow consistent with the intermittency in realistic flows.

It is also well-known that the GOY model exhibits a static solution consisting of cyclic oscillations involving three consecutive shells with respect to the shell index (as shown in [40]), which overlap with the scaling of the structure function, making the estimation of scaling laws less accurate. It is possible to filter out these oscillations [21], by studying the scaling behavior of the quantity constructed in terms of three point correlations as follows:

$$\Sigma_{n,p} = \left\langle \left| \text{Im} (u_{n-1}^* u_n^* u_{n+1}^*) \right|^{p/3} \right\rangle$$

We can characterize the intermittency the same way in our model, and compare it with the intermittency in the standard GOY case. Note that this is a more stringent test, and a potentially more interesting comparison since the Fibonacci sequence shell model breaks the exact self-similar structure of the GOY model. As can be seen in the inset plot of Figure 4, the scaling of Σ_p is not affected by these three-point oscillations, therefore it allows for a slightly more accurate estimation of the scaling exponents.

The scaling exponent $\xi(p)$ of the structure function of order p can also be estimated via an extended self simi-

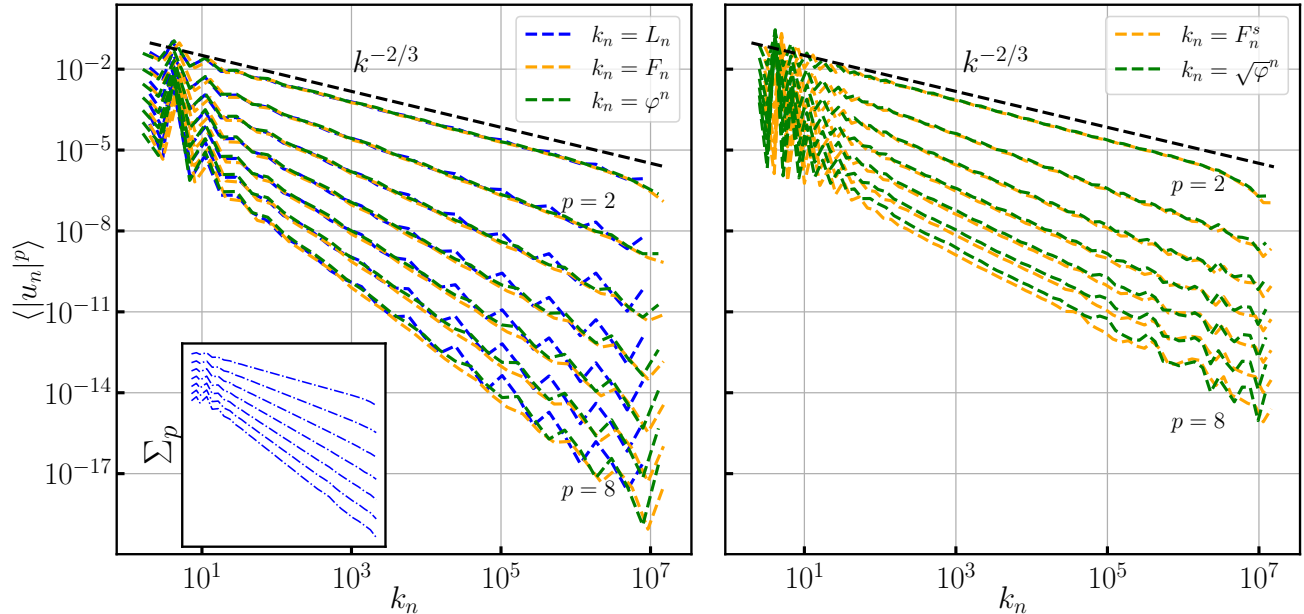


Figure 4. Log-log plot of the structure functions of order p (from two to eight, top to bottom), defined as $S_p(k_n) = \langle |u(k_n)|^p \rangle$ as a function of the wave-number k_n , for both the self similar spaced model and the asymptotically self similar one in two different spacing considered, the golden ratio and the square root of the golden ratio. The inset plot indicates the structure function after eliminating the periodic three oscillations, showing the scaling of the quantity Σ_p .

larity (ESS) procedure [41] that allows an improved determination of the intermittency, due to the reduction of eventual subdominant contributions to the scaling: through a linear fit of the ordinate as a function of the abscissa in a log-log plot of the structure function S_p or Σ_p as a function of the third order structure function $S_{p=3}$ ($\Sigma_{p=3}$), assuming a power law scaling of the form $S_p(k_n) \sim S_3^{-\xi(p)}$ ($\Sigma_p(k_n) \sim \Sigma_3^{-\xi(p)}$) in the inertial range, selecting a range of shells that correspond to a perfectly constant flux, as can be seen for different values of p in Figure 5.

As previously noted, spacings smaller than the golden ratio, where actual triadic interactions are possible with the shell centers, such as the square root of golden ratio spacing or the plastic ratio spacing, be it on an exactly or asymptotically self-similar model, appear to exhibit behavior that does not align perfectly with the Kolmogorov scaling, suggesting higher-order corrections. First, the quantities $\langle |u_n|^p \rangle$ are shown in Figure 4 for shell models with golden ratio and the square root of golden ratio spacings. This demonstrates that the scaling behavior for these two different types of spacing is significantly different, while indicating no substantial differences from a given integer sequence and their corresponding self-similar counterpart.

The scaling factors $\xi(p)$ that are estimated through an ESS procedure are plotted in Figure 6 as a function of p , the order of the structure function, in order to quantify the intermittency corrections for all the sequences that

have been studied. As usual, the deviation from the linear scaling serves as a measure of intermittency. Note that we have also performed the simpler procedure of fitting the structure functions directly and the results were essentially the same.

First, we note that all the curves clearly exhibit very high deviations from what would be a mono-fractal scaling, which may be interpreted as extremely high levels of intermittency. In addition, for each family of curves, i.e., for every asymptotic scaling ratio, we can observe that the intermittency of the integer sequences follows closely the GOY version with that scaling, within the error bars of the fitting procedure and the slight differences in injection and dissipation. However, we note an interesting, and somewhat unexpected result: for each family of series, intermittency follows a different trend, suggesting that smaller shell spacing corresponds to larger intermittency corrections.

Additionally, we perform an analysis of intermittency over time, following the approach outlined in Ref. [13, 42, 43], which we do not present here, but which shows similar trends. We find that the presented results are relatively robust with clear scaling laws demonstrated by the structure functions, having tested three different series for each asymptotic scaling factors. These results are non-trivial and quite novel, considering that Sabra and shell models have traditionally been explored numerically with an inter-shell spacing of $g = 2, \varphi$, and that smaller shell spacing have been examined only in a few examples

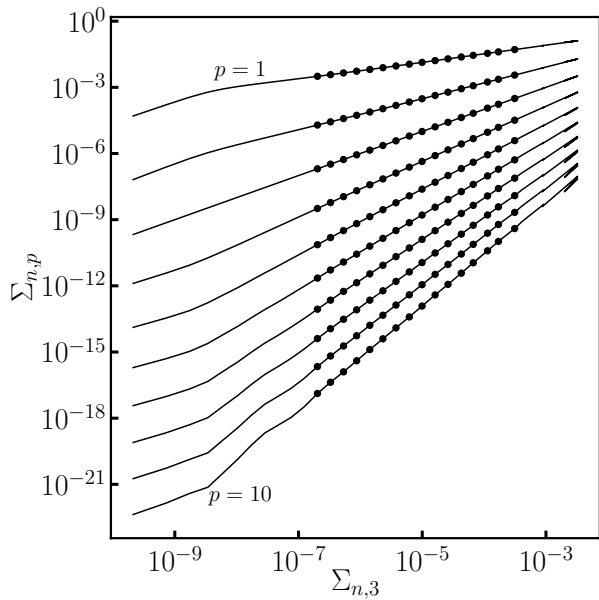


Figure 5. In the figure, for the Fibonacci sequence case, we illustrate the procedure for estimating the scaling exponents $\xi(p)$ following the ESS method. The scalings of the quantity Σ_p are plotted as a function of Σ_3 . The structure function $p = 1, 2, \dots, 10$ are displayed from top to bottom. The dots represent the set of points used for the fitting procedure, corresponding to approximately four decades in the inertial range, which aligns with the constant flux window.

([21, 44, 45]). An in-depth characterization of the intermittency dependence on varying inter-shell spacing of standard shell models is beyond the scope of the present paper, whose primary goal is to demonstrate the robustness of the implementation of shell models on recurrent sequences, leaving a more thorough investigation of the former for a future publication.

D. A two sequence compound example

In this section, we demonstrate the behavior of the proposed model on a two-sequence compound constructed by merging two sequences. As a particular example, we consider the compound formed by the union of the Fibonacci and Lucas numbers. These two sequences share the same recurrence relations, and the same asymptotic scaling factor, the golden ratio. The Fibonacci and Lucas sequences are complementary, and one can construct similar spirals that rotate in co and counter-clockwise directions from them respectively, which for large numbers, approximate golden spirals common also in pattern formation in plants such as phyllotaxis [46]. In this sense, it is a compound sequence: and the two sequences asymptotically share the same self-similar spacing, i.e. the golden number, they begin with slightly different

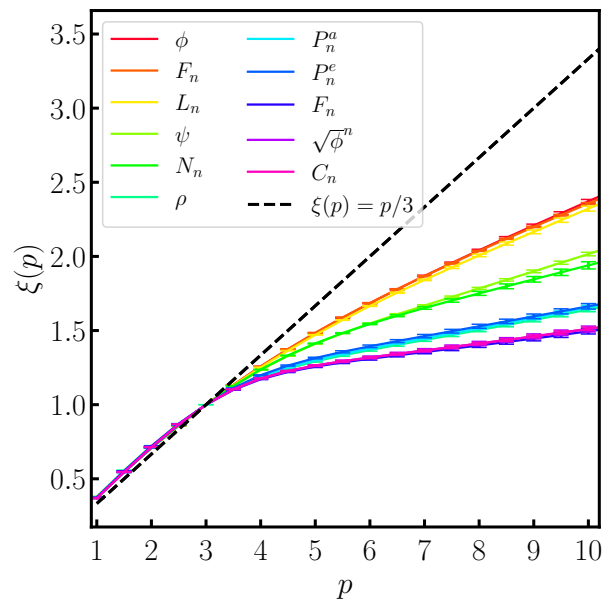


Figure 6. Plot of the scaling exponent $\xi(p)$ as a function of the order of the structure function estimated via the ESS procedure for all the sequences and corresponding self-similar sequences studied, the parameters utilized corresponds to what displayed in table I. The dashed line correspond to the Kolmogorov scaling $\xi(p) = p/3$.

numbers but grow with the same scaling factor, thus not overlapping but forming a new sequence that can be expressed as:

$$\{\dots F_n, L_{n-1}, F_{n+1}, L_n, F_{n+2}, L_{n+2}, \dots\}$$

Consequently, the shell model constructed in the asymptotic limit does not converge to a constant inter-shell ratio. Instead, the inter-shell ratio alternates between two values:

$$\frac{k_{n+1}}{k_n} = \begin{cases} \frac{F_{n+2}}{L_n} = \frac{\varphi^2}{\sqrt{5}} \simeq 1.171 \\ \frac{L_n}{F_{n+1}} = \frac{\sqrt{5}}{\varphi} \simeq 1.382 \end{cases}$$

Considering two consecutive shells lumped together as one, the inter-shell spacing would approach the golden ratio. Note also that there are two kinds of triads in the compound. The first triad with L_n as the central node is an acute triangle with the asymptotic angles $\theta_{kq} = 37.92^\circ$, $\theta_{kp} = 83.94^\circ$ and $\theta_{pq} = 58.14^\circ$, and the second one with F_n as the central node is an obtuse one with the angles $\theta_{kq} = 37.92^\circ$, $\theta_{kp} = 96.06^\circ$ and $\theta_{pq} = 46.02^\circ$.

We note that this type of construction has emerged in previous results [28], which developed a model based on a decimation of Fourier space using the vertices of nested polyhedra, allowing for the existence of genuine triad conditions among three modes belonging to three consecutive “shells”: the compound in this case was formed by a

sequence of consecutive dodecahedron-icosahedron structures, scaled by the golden ratio. In this type of decimation, the inter-shell ratio alternates due to the differing scaling factors between the icosahedron and the dodecahedron.

Remarkably, in this particular type of Fourier space decimation, the nested polyhedra model shows no sign of intermittency. Therefore, implementing a compound sequence in a 1D chain is intriguing, especially given the trends observed in the previous section on asymptotically self-similar sequences: smaller spacing tends to indicate an increase in intermittency corrections. *A priori*, it is unclear whether the model will exhibit a level of intermittency comparable to that observed in the Fibonacci sequence or similar to the one found in sequences with smaller inter-shell spacing, or have no intermittency as in the case of nested polyhedra models.

As shown in Figure 7, the model implemented on the compound sequence reproduces results consistent with Kolmogorov scaling. The spectrum shows the same features observed in other cases, such as oscillations at the forcing scale and smaller in the inertial range. These oscillations are analogous to the period-three oscillations of the standard GOY model. However, we note that the 1D map that generates the stationary inviscid solution [40] is modified by the fact that the shell wave-numbers are not asymptotically regular. The energy flux remains remarkably constant in the inertial range, which also serves to demonstrate that the proposed nonlinear term (2) generalizes the usual GOY model on arbitrary sequences of wave-numbers.

Regarding the intermittency, it is interesting to note that the scaling of $\xi(p)$, as shown in Figure 6, displays a scaling behavior very similar to that observed for the two series with a spacing of the square root of the golden ratio (exactly or asymptotically). Actually, if we take the geometric mean of the two inter-shell ratios, we obtain the square root of the golden ratio. Therefore, we hypothesize that, also in the compound sequence case, the level of intermittency is determined merely by the spacing. Specifically, in the sense that it is the average spacing of the sequence of shells that determines the level of intermittency. It is puzzling however, how one goes from that, to “no intermittency” in the case of the nested polyhedra model, suggesting that the phase dynamics on the constrained 1D chain structure of the shell model has something to do with the observed dependency of the intermittency to shell spacing. Again a detailed exploration of this observation, is left to a future publication.

Note finally that the compound, which we argue to correspond to an integer series version of the nested polyhedra with its alternating triads, can also be used to construct a recurrent series version of the log-lattice. Given that $L_n = F_{n-1} + F_{n+1}$ and $5F_n = L_{n+1} - L_{n-1}$, this results in more triads per node (i.e. 18 for Fibonacci, to 32 and 50 for the compound), and more “non-local” interactions.

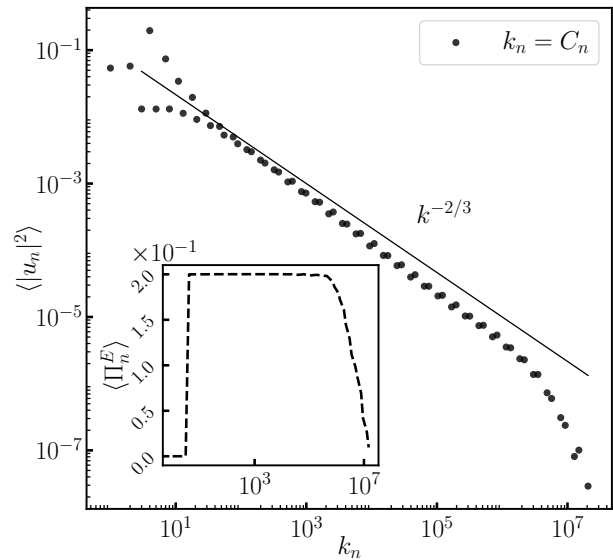


Figure 7. Log-log plot of the energy spectra as function of the wave-number k_n for the compound sequence case. The inset semi-log plot represents the spectral energy flux.

III. HELICAL SHELL MODELS ON A RECURRENT SEQUENCE

In the previous section, a generalization of the conventional GOY model to generic wave-number sequences, which are in practice obtained from recurrence relations and have asymptotically self-similar structures is proposed. It is demonstrated that shell models on such recurrent sequences exhibit standard features of conventional shell models such as power law spectra, constant spectral flux, and intermittency. A particular form of the interaction coefficients were used for this purpose, which guarantees conservation of energy and helicity as in the original equations.

However, in line with the usual convention in shell models, the helicity in this picture was defined as $H = \sum_n (-1)^n k_n |u_n|^2$, which allows one to enforce the conservation of a non-positive defined invariant that scales as helicity, but does not in fact correspond to it in any meaningful sense. Therefore, if we want to account for the complex role played by helicity in turbulent cascade [47–51], it is necessary to generalize the model to include a conserved non-positive defined invariant that is closer to the usual definition of helicity, as derived from the Navier-Stokes equations.

In order to achieve this, we can use the so called helical decomposition [52], and following De Pietro *et al.* [53], write a set of arbitrarily elongated shell models, but on a recurrent sequence in accordance with the models considered above. The resulting model evolves two shell variables u_n^+ and u_n^- , with respectively positive and negative helicities and allows us to define energy and helicity

as follows:

$$E = \sum_n |u_n^+|^2 + |u_n^-|^2, \quad H = \sum_n k_n (|u_n^+|^2 - |u_n^-|^2) \quad (5)$$

The general form of the shell model, omitting the dissipative and forcing terms, with arbitrary elongation can be written in compact form as:

$$\frac{du_n^{s_0}}{dt} = s_0 (a_n u_{n+\ell+m}^{s_3^*} u_{n+\ell}^{s_1^*} + b_n u_{n-\ell}^{s_1^*} u_{n+m}^{s_2^*} + c_n u_{n-m}^{s_2^*} u_{n-\ell-m}^{s_3^*})$$

with

$$\begin{aligned} a_n &= Q \frac{s_1}{s_0} \left(\frac{s_2}{s_0} k_{n+\ell+m} - k_{n+\ell} \right) \\ b_n &= Q \left(\frac{s_1}{s_0} k_{n-\ell} - \frac{s_2}{s_0} k_{n+m} \right) \\ c_n &= Q \frac{s_2}{s_0} \left(k_{n-m} - \frac{s_1}{s_0} k_{n-\ell-m} \right) \end{aligned}$$

$s_3 \equiv s_0 s_1 s_2$, and where $Q = Q_{\ell m} (s_1/s_0, s_2/s_0)$ is the geometric factor of the triad class that is considered. The four triad classes can be defined as the 4 possible combinations of the signs of s_1/s_0 and s_2/s_0 . In practice for a given set of wave-vectors $p < k < q$ which in this case corresponds to $p = k_{n-\ell}$ and $q = k_{n+m}$, it can be written as:

$$\begin{aligned} Q &\equiv Q_{kpq}^{s_0 s_1 s_2} = Q \left(\frac{p}{k}, \frac{s_1}{s_0}, \frac{q}{k}, \frac{s_2}{s_0} \right) \\ &= \frac{s_1 s_2}{s_0 s_0} \sin(\alpha + \beta) \left(1 + \frac{s_1 p}{s_0 k} + \frac{s_2 q}{s_0 k} \right) \end{aligned}$$

where α and β are the angles between k and p and k and q respectively, which can be written as usual as:

$$\begin{aligned} \alpha &= \arccos \left(\frac{q^2 - k^2 - p^2}{2kp} \right) \\ \beta &= \arccos \left(\frac{p^2 - k^2 - q^2}{2qk} \right) \end{aligned}$$

Notice that, by choosing $g = 2$, $\ell = 1$, $m = 1$, we obtain the simple helical shell model discussed by Benzi *et al.* [45]. However the general form of the model allows all kinds of models with non-local interactions.

It can be shown that the proposed form of the helical shell model, conserves energy and helicity. One can also put all the 4 classes of interactions together by considering a sum over triad classes on the right hand side, with the corresponding geometric factors for each class as discussed in Ref. [54] for local interactions. Note that even though, on a recurrent sequence, the actual geometric factors are not exactly the same, and in the above form we take them to be the same, the energy and helicity are still properly conserved. This is non-trivial if one thinks

in terms of conventional shell models and self-similarity. However it becomes trivial if one thinks in terms of a chain of triads, each triad conserves energy separately regardless of the exact geometric factor, so as long as one keeps all the nodes of each triad that is considered and all the geometric factors of a triad remain the same (it doesn't matter if the actual value of the geometric factor may be a bit off), all the conservation laws of the original system will continue to be respected.

Note that here, we presented a general helical shell model based on the symmetries of the helically decomposed turbulence. Below we will consider a particular class and range of interactions and show that in a particular configuration, such a model can give rise to inverse cascade. However, in order to make connection to the GOY model, consider alternatively the class 4, which is defined by the relations $s_1/s_0 = s_2/s_0 = -1$. This means that the middle wave-number is of opposite chirality to the other two, and therefore we can setup two chains of nodes with alternating chiralities that never interact. In the first chain, the even nodes would be $+$ and odd ones would be $-$, in the second chain the odd nodes would be $+$ and even ones would be $-$. This explains the usual interpretation of the helicities carried by shell variables in the GOY model.

A. Inverse cascade on a recurrent sequence

In this section, we present the numerical implementation of the helical shell model on a recurrent wave-number sequence, in order to demonstrate that the agreement between the recurrent and self-similar shell model is not model dependent.

Helically decomposed shells model have been studied in the case of local interactions, both in a 1D chain of interacting modes and in hierarchical trees in Ref. [45, 55]. It is also interesting to note, in accordance with the results of the previous section, that in Ref. [44], a particular class of helical shell model shows that a decrease in the inter-shell spacing leads to a reduction in intermittency corrections.

More recently non-local interactions have been included in the shell model formulation in Ref. [53, 54]. The nontrivial aspect of including non-local couplings, arises from a class of heterochiral interactions, namely $s_1/s_0 = -1$, $s_2/s_0 = +1$, which for sufficiently elongated triads drive an inverse cascade. The transition from direct to inverse cascade was first predicted by Waleffe [47, 52] at the threshold value $p/k < 0.278$ (assuming $p < k < q$) in the shape of the triad interaction, and numerically confirmed by De Pietro *et al.* [53]. The inverse cascade the helical shell model represents an anomaly, as it is well known that constructing a shell model that conserves the inviscid invariants of 2D turbulence, namely energy and enstrophy, the inverse cascade range is typically dominated by an equipartition spectrum as observed in Ref. [56–58]. The interplay between equilib-

rium and cascades solutions as been further investigated by Ditlevsen and Mogensen [57], Gilbert *et al.* [59], Tom and Ray [60].

We implement the helical shell model formulation on Lucas and Fibonacci sequences and the corresponding self similar spaced model, in a numerical setup capable of demonstrating an inverse energy cascade. Thus, we cover seven decades with $N = 36$ shells, and in order to drive an inverse cascade $s_1/s_0 = -1, s_2/s_0 = +1$ and $l = 3$, $m = 1$, resulting asymptotically in $p/k \approx 1/\varphi^3 \approx 0.236$, which satisfies the inequality predicted by Waleffe.

The system is driven by small scale random forcing acting on two consecutive shells, $n_f = 32, 33$. The forcing amplitude is unbalanced between the shells carrying positive and negative helicities, with $f^+ = f$, $f^- = 1/2f$, where we set $f = 0.8$. The dissipative term $d_n = \nu k_n^{2p} + \mu k_n^{-2q}$, has the form of a small scale dissipation, with $\nu = 4 \cdot 10^{-12}$, $p = 1$, and a large scale hypo-viscosity with $\mu = 1$, $q = 2$, in order to prevent energy accumulation on the first shells.

As shown in Fig. 8, by forcing the system at small scales an inverse energy cascade develops for sufficiently elongated triads. We observe how the energy spectrum is in good agreement with the inverse energy cascade prediction for both Lucas and Fibonacci sequences and the corresponding self-similar sequence, with three models overlapping in the inertial range. However the energy of the first few shells differ, mainly due to the role played by hypoviscosity: variations in the first wave numbers between the sequences, result in different damping effects.

The flux due to nonlinear terms across the n -th shell can be defined by as:

$$\Pi_n^E = \sum_{j=1}^n 2Im \left(u_j^{+*} \frac{d}{dt} u_j^{+*} \Big|_{nl} + u_j^{-*} \frac{d}{dt} u_j^{-*} \Big|_{nl} \right), \quad (6)$$

where the subscript nl denote the nonlinear terms. The spectral fluxes for the inverse cascade on the different sequences that are considered are shown in the inset plot of Fig. 8. We note that the negative flux remains perfectly constant within the inertial range, as obtained for the GOY model implementation. The magnitude of the flux differs slightly between the Fibonacci and the other two sequences coincide, as the energy injection varies due to the differences in the shell wave numbers: asymptotically, the wave numbers $k_n = \varphi^n$ align with the Lucas sequence, but is shifted with respect to the Fibonacci sequence, even though all sequences converge to the same inter-shell spacing. The negative flux exhibits a cusp in all three models around the fourth shell, where do to the elongation of the triad $l = 3$ the term $n - l$ reach the boundary.

We conclude that, also for the helically decomposed shell model, the behavior on the recurrent integer sequences shows no significant differences compared to that on the corresponding self-similar scaling.

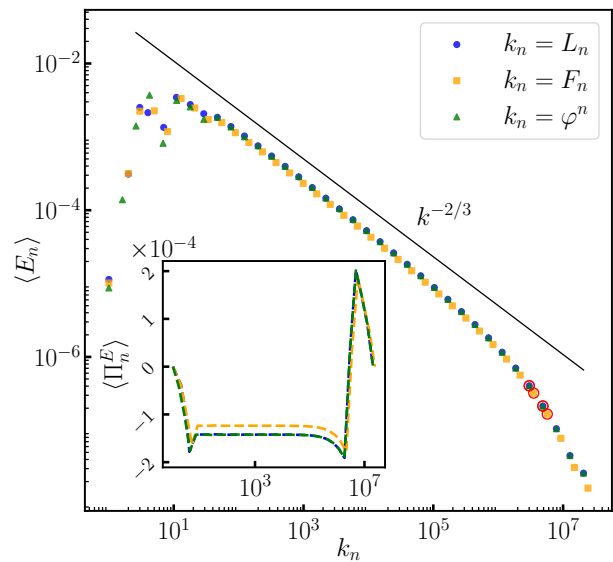


Figure 8. Log-log plot of the spectral energy for each shell $\langle |u_n^+|^2 + |u_n^-|^2 \rangle$ as a function of the wave-number k_n , for a wave-number sequences corresponding to the Fibonacci numbers, Lucas numbers and the respective self-similar spacing $k_n \propto \varphi^n$. For each sequence the two shells where the forcing acts are marked with a red circle. In the inset, a semi-log plot shows the spectral energy flux $\langle \Pi_n^E \rangle$ due to nonlinear terms defined in Eq. (6), as a function of the wave-number k_n (log. scale).

IV. CONCLUSION

Considering shell models as prototypes or building blocks of a whole host of reduced models, we propose a natural generalization of the GOY model (i.e. with $g = 2$, hence on a recurrent sequence of powers of two), into *other* recurrent sequences, including Fibonacci, Lucas, Padovan and Narayana series and their combinations, which can be constructed from simple additive recurrence relations (such as $k_n = k_{n-1} + k_{n-2}$). Such series tend to generate integer numbers that are asymptotically self-similar (i.e. $k_{n+1}/k_n \approx k_n/k_{n-1} \approx g$ for $n \gg 1$).

Considering a particular form of the interaction coefficients, a model can be constructed that respects the conservation laws of the original system regardless of the shell spacing. This allows the implementation of shell models on recurrent sequences characterized by different asymptotic inter-shell spacing, and their comparison to the conventional shell models with a constant g equal to the asymptotic ratio showed no substantial differences. In particular, the intermittency analysis on various sequences show how the deviation from the Kolmogorov scaling are determined by the inter shell spacing rather than whether or not the model is on a recurrent sequence or have constant logarithmic spacing. It was observed in particular that smaller spacings lead to higher appar-

ent intermittency as defined in the usual way. Suggesting that burst-like solutions, to which the GOY model is prone in the continuum limit [61], may be an explanation of the apparent high intermittency with small inter-shell spacing.

The particular case of the compound sequence, clearly demonstrates how the proposed model is robust, showing a spectral behavior in accordance with the regular GOY model, even though the inter-shell spacing in such a model alternates even for large n . The intermittency corrections are comparable to those obtained for a self-similar model with a spacing equal to the geometric mean of the two alternating spacings, suggesting again that in a constrained 1D chain of interacting modes, phase dynamics approaching the continuum limit is the key mechanism of intermittency in shell models.

In addition to these additive recurrence relations, we have also considered what we call the square root of Fibonacci numbers sequence, which follows a recurrence that one obtains by rounding the squares of the sums of the last two elements to the nearest integer (i.e. $k_n = \lfloor \sqrt{k_{n-1}^2 + k_{n-2}^2} \rfloor$). Like the other series with $g < \varphi$, such series allow actual triads, and hence can be used for example to construct logarithmically discretized models, where the discretization in the magnitude would be constructed from the recurrence relations, while the angular discretization would be linear.

Finally, with the same objective, we presented the formulation of a helically decomposed shell model on a recurrent wave-number sequence with generic elongations and helical interactions classes, generalizing the work of [53, 54]. We tested this construction by demonstrating an inverse energy cascade on a recurrent sequence, which validates the previous observation that shell models on recurrent sequences display the same characteristics as standard shell models.

It is also worth re-iterating that the primary motivation of this work has been to make the connection between regular and logarithmic discretization used in turbulence modeling. By showing that this can be achieved by recurrent sequences in shell models, paves the way to applying the same principle to other logarithmically discretized systems, such as log-lattices, LDM models, nested-polyhedra models etc. It can be shown for ex-

ample that using the Fibonacci or the Lucas sequences, a log-lattice formulation would result in 18 triads per wave-number element (at least two of which are flat triads), whereas if one used the compound sequence made up of both Lucas and Fibonacci numbers, the number of triads goes up to 32 for Fibonacci nodes, and 50 for Lucas nodes. Note that recurrent sequences would also allow a nice transition from a regular grid, $k_{xi} = \frac{2\pi}{L_x} [1, 2, 3, 4, 5, n_x - 2, n_x - 1]$ to an asymptotically logarithmic one, using the recurrence relation on the last few nodes of the grid elements, (e.g. $k_{n_x} = k_{n_x-1} + k_{n_x-2}$). Unfortunately the details of such an implementation is out of scope of the current paper and is left to a future publication.

Also, the application of the idea to other models, such as the nested polyhedra model, where one “shell” is represented by an icosahedron-dodecahedron compound whose vertices have x, y, z components which can be written basically using combinations of $1, \pm\varphi, \pm\varphi^2$ so that exact triadic interactions are possible among them, can be replaced by versions of these objects where each components can be constructed using recurrent series, such as the Fibonacci series, which would approach asymptotically to perfect icosahedron-dodecahedron compounds.

ACKNOWLEDGMENT

The authors would like to thank Dr. Benjamin Favier of IRPHE-Aix Marseille University, for bringing this issue to our attention and the pointing out the interest in the numerical community for such a study. The authors would also like to thank the Isaac Newton Institute for Mathematical Sciences, Cambridge, for support and hospitality during the programme “Anti-diffusive dynamics: from sub-cellular to astrophysical scales” during which these discussions took place. This work has benefited from a grant managed by the Agence Nationale de la Recherche (ANR), as part of the program ‘Investissements d’Avenir’ under the reference (ANR-18-EUR-0014) and has been carried out within the framework of the EUROfusion Consortium, funded by the European Union via the Euratom Research and Training Programme (Grant Agreement No 101052200 — EUROfusion) and within the framework of the French Research Federation for Fusion Studies.

-
- [1] U. Frisch, *Turbulence: The Legacy of A. N. Kolmogorov* (Cambridge University Press, Cambridge, 1995).
 - [2] G. Falkovich, *J. Phys. A* **42**, 123001 (2009).
 - [3] H. Rose and P. Sulem, *Journal de Physique* **39**, 441 (1978).
 - [4] T. Bohr, M. H. Jensen, G. Paladin, and A. Vulpiani, *Dynamical Systems Approach to Turbulence*, Cambridge Nonlinear Science Series (Cambridge University Press, 1998).
 - [5] V. N. Desnianskii and E. A. Novikov, *J. Appl. Math. Mech.* **38**, 468 (1974).
 - [6] M. Yamada and K. Ohkitani, *Progress of Theoretical Physics* **79**, 1265 (1988).
 - [7] V. S. L’vov, E. Podivilov, A. Pomyalov, I. Procaccia, and D. Vandembroucq, *Phys. Rev. E* **58**, 1811 (1998).
 - [8] L. Biferale, *Ann. Rev. Fluid Mech.* **35**, 441 (2003).
 - [9] P. D. Ditlevsen, *Turbulence and Shell Models* (Cambridge University Press, 2010).

- [10] L. Biferale, G. Boffetta, A. Celani, and F. Toschi, *Physica D: Nonlinear Phenomena* **127**, 187 (1999).
- [11] R. Benzi, L. Biferale, and G. Parisi, *Physica D: Nonlinear Phenomena* **65**, 163 (1993).
- [12] L. Biferale, M. Cencini, D. Pierotti, and A. Vulpiani, *Journal of Statistical Physics* **88**, 1117 (1997).
- [13] S. S. Ray, D. Mitra, and R. Pandit, *New J. Phys.* **10**, 033003 (2008).
- [14] Y. Hattori, R. Rubinstein, and A. Ishizawa, *Phys. Rev. E* **70**, 046311 (2004).
- [15] M. H. Jensen, G. Paladin, and A. Vulpiani, *Phys. Rev. A* **45**, 7214 (1992).
- [16] A. Kumar and M. K. Verma, *Phys. Rev. E* **91**, 043014 (2015).
- [17] F. Plunian and R. Stepanov, *New Journal of Physics* **9**, 294 (2007).
- [18] F. Plunian, R. Stepanov, and P. Frick, *Phys. Rep. - Rev. Sect. Phys. Lett.* **523**, 1 (2013).
- [19] A. Verdini and R. Grappin, *Phys. Rev. Lett.* **109**, 025004 (2012).
- [20] V. Berionni, P. Morel, and Ö. D. Gürçan, *Physics of Plasmas* **24**, 122310 (2017).
- [21] L. Kadanoff, D. Lohse, J. Wang, and R. Benzi, *Phys. Fluids* **7**, 617 (1995).
- [22] D. Pisarenko, L. Biferale, D. Courvoisier, U. Frisch, and M. Vergassola, *Physics of Fluids A* **5**, 2533 (1993).
- [23] Ö. D. Gürçan, S. Xu, and P. Morel, *Phys. Rev. E* **100**, 043113 (2019).
- [24] Ö. D. Gürçan, P. Morel, S. Kobayashi, R. Singh, S. Xu, and P. H. Diamond, *Phys. Rev. E* **94**, 033106 (2016).
- [25] C. S. Campolina and A. A. Mailybaev, *Phys. Rev. Lett.* **121**, 064501 (2018).
- [26] C. S. Campolina and A. A. Mailybaev, *Nonlinearity* **34**, 4684 (2021).
- [27] G. Costa, A. Barral, and B. Dubrulle, *Phys. Rev. E* **107** (2023), 10.1103/PhysRevE.107.065106.
- [28] Ö. D. Gürçan, *Phys. Rev. E* **95**, 063102 (2017).
- [29] Ö. D. Gürçan, *Phys. Rev. E* **97**, 063111 (2018).
- [30] K. Ohkitani and M. Yamada, *Progress of Theoretical Physics* **81**, 329 (1989).
- [31] A. A. Mailybaev, *Phys. Rev. Fluids* **7**, 034604 (2022).
- [32] S. Aumaitre and S. Fauve, *Phys. Rev. Lett.* **132**, 114002 (2024).
- [33] Z.-S. She and E. Leveque, *Phys. Rev. Lett.* **72**, 336 (1994).
- [34] N. Vladimirova, M. Shavit, and G. Falkovich, *Phys. Rev. X* **11**, 021063 (2021).
- [35] C. Rackauckas, “Sciml/differentialequations.jl: v7.14.0,” (2024).
- [36] C. A. Kennedy and M. H. Carpenter, *Applied Numerical Mathematics* **44**, 139 (2003).
- [37] J. Bezanson, A. Edelman, S. Karpinski, and V. B. Shah, *SIAM Review* **59**, 65 (2017), <https://doi.org/10.1137/141000671>.
- [38] M. H. Jensen, G. Paladin, and A. Vulpiani, *Phys. Rev. A* **43**, 798 (1991).
- [39] X. M. de Wit, G. Ortali, A. Corbetta, A. A. Mailybaev, L. Biferale, and F. Toschi, *Phys. Rev. E* **109**, 055106 (2024).
- [40] L. Biferale, A. Lambert, R. Lima, and G. Paladin, *Physica D: Nonlinear Phenomena* **80**, 105 (1995).
- [41] R. Benzi, S. Ciliberto, R. Tripiccion, C. Baudet, F. Massaioli, and S. Succi, *Phys. Rev. E* **48**, R29 (1993).
- [42] D. Mitra and R. Pandit, *Phys. Rev. Lett.* **93**, 024501 (2004).
- [43] R. Pandit, S. S. Ray, and D. Mitra, *Eur. Phys. J. B* **64**, 463 (2008).
- [44] R. Benzi, L. Biferale, and E. Trovatore, *Phys. Rev. Lett.* **77**, 3114 (1996).
- [45] R. Benzi, L. Biferale, R. M. Kerr, and E. Trovatore, *Phys. Rev. E* **53**, 3541 (1996).
- [46] A. C. Newell, P. D. Shipman, and Z. Sun, *Journal of Theoretical Biology* **251**, 421 (2008).
- [47] F. Waleffe, *Physics of Fluids A: Fluid Dynamics* **5**, 677 (1993).
- [48] L. Biferale, S. Musacchio, and F. Toschi, *J. Fluid Mech.* **730**, 309 (2013).
- [49] A. Alexakis, *J. Fluid Mech.* **812**, 752 (2017).
- [50] A. Alexakis and L. Biferale, *Physics Reports* **767-769**, 1 (2018), cascades and transitions in turbulent flows.
- [51] G. Sahoo and L. Biferale, *Fluid Dyn. Res.* **50** (2018), 10.1088/1873-7005/aa839a.
- [52] F. Waleffe, *Physics of Fluids A: Fluid Dynamics* **4**, 350 (1992).
- [53] M. De Pietro, L. Biferale, and A. A. Mailybaev, *Phys. Rev. E* **92**, 043021 (2015).
- [54] N. M. Rathmann and P. D. Ditlevsen, *Phys. Rev. E* **94** (2016), 10.1103/PhysRevE.94.033115.
- [55] R. Benzi, L. Biferale, R. Tripiccion, and E. Trovatore, *Phys. Fluids* **9**, 2355 (1997), https://pubs.aip.org/aip/pof/article-pdf/9/8/2355/19261896/2355_1_online.pdf.
- [56] E. Aurell, G. Boffetta, A. Crisanti, P. Frick, G. Paladin, and A. Vulpiani, *Phys. Rev. E* **50**, 4705 (1994).
- [57] P. Ditlevsen and I. Mogensen, *Phys. Rev. E* **53**, 4785 (1996).
- [58] E. Aurell, P. Frick, and V. Shaidurov, *Physica D: Nonlinear Phenomena* **72**, 95 (1994).
- [59] T. Gilbert, V. L’vov, A. Pomyalov, and I. Procaccia, *Phys. Rev. Lett.* **89** (2002), 10.1103/PhysRevLett.89.074501.
- [60] R. Tom and S. S. Ray, *EPL* **120** (2017), 10.1209/0295-5075/120/34002.
- [61] K. Andersen, T. Bohr, M. Jensen, J. Nielsen, and P. Olesen, *Physica D* **138**, 44 (2000).